Cardiovascular Innovations and Applications

Vol. 9 (2024) 1
ISSN 2009-8618
DOI 10.15212/CVIA.2023.0079

RESEARCH ARTICLE

Incremental Metabolic Benefits from Cryoablation for Paroxysmal Atrial Fibrillation: Insights from Metabolomic Profiling

Mengjie Xie, MD[1–7,a], Fuding Guo, MD[1–7,a], Jun Wang, MD[1–7,a], Yijun Wang, MD[1–7], Zhihao Liu, MD[1–7], Jing Xie, MD, PhD[1–7], Zhuo Wang, MD, PhD[1–7], Songyun Wang, MD, PhD[1–7], Liping Zhou, MD, PhD[1–7], Yueyi Wang, MD, PhD[1–7], Hong Jiang, MD, PhD[1–7] and Lilei Yu, MD, PhD[1–7]

[1]*Department of Cardiology, Renmin Hospital of Wuhan University, Wuhan 430060, P.R. China*
[2]*Institute of Molecular Medicine, Renmin Hospital of Wuhan University, Wuhan 430060, P.R. China*
[3]*Hubei Key Laboratory of Autonomic Nervous System Modulation, Wuhan 430060, P.R. China*
[4]*Taikang Center for Life and Medical Sciences, Wuhan University, Wuhan 430060, P.R. China*
[5]*Cardiac Autonomic Nervous System Research Center of Wuhan University, Wuhan 430060, P.R. China*
[6]*Hubei Key Laboratory of Cardiology, Wuhan 430060, P.R. China*
[7]*Cardiovascular Research Institute, Wuhan University, Wuhan 430060, P.R. China*

Received: 10 July 2023; Revised: 25 September 2023; Accepted: 16 October 2023

Abstract

Background: Cryoablation (CRYO) is a novel catheter ablation technique for atrial fibrillation (AF). However, uncertainty persists regarding the role of metabolic modifications associated with CRYO. This study was aimed at exploring whether CRYO influences the metabolic signature – a possibility not previously investigated.
Methods: Paired serum samples from patients with AF (n = 10) were collected before and 24 h after CRYO. Untargeted metabolomic analysis was conducted with LC-MS. Univariate and multivariate analyses were applied to identify differential metabolites between samples. Pathway enrichment and Pearson correlation analyses were performed to reveal the perturbed metabolic pathways and potential interactions.
Results: Levels of 19 metabolites showed significant changes between baseline and 24 h after CRYO. Pathway analysis revealed that the perturbed metabolites were enriched in unsaturated fatty acid biosynthesis, retrograde endocannabinoid signaling, and neuroactive ligand-receptor interactions. Pearson correlation analysis indicated strong correlations among differential metabolites, biochemical markers, and clinical indicators.
Conclusions: CRYO induces systemic changes in the serum metabolome in patients with paroxysmal AF and provides potential metabolic benefits. Our findings might enable enhanced understanding of the pathophysiology and metabolic mechanisms involved in catheter ablation.

Keywords: cryoablation; metabolomics; atrial fibrillation; polyunsaturated fatty acids; neuroactive ligand-receptor interaction pathways

©2024 Cardiovascular Innovations and Applications. Creative Commons Attribution-NonCommercial 4.0 International License

Introduction

Atrial fibrillation (AF), the most prevalent sustained cardiac arrhythmia in adults, has occurred in 43.6 million cases worldwide in 2016 and tends to affect older age groups [1]. Pulmonary vein isolation (PVI) is a safe and effective treatment for patients with AF. Cryoablation (CRYO) is a novel catheter ablation technique that has emerged as an effective and fundamental therapeutic strategy for PVI in patients with paroxysmal AF [2, 3]. Recent studies have shown that initial treatment with cryoablation in patients with paroxysmal AF is more effective than drug therapy, thus resulting in a lower incidence of atrial arrhythmias and a lower AF burden at 3-year follow-up than observed with initial use of antiarrhythmic drugs [4]. The main principle of CRYO is freezing of the ablation site through the endothermic process of evaporation of liquid nitrous oxide, thus damaging the tissue surrounding the pulmonary veins in contact with the balloon and forming a continuous ring of transmural injury that isolates the pulmonary veins [5].

The main metric of CRYO success is the disappearance of the pulmonary vein potential immediately after freezing. However, other potential benefits of CRYO treatment beyond electrophysiological parameters are not fully understood. Extensive evidence indicates that cold exposure enhances brown adipose tissue (BAT) activity, and that the high metabolic/thermogenic activity of brown fat regulates lipid and glucose metabolism, while consuming energy by accelerating the uptake and utilization of various metabolic substrates, including glucose, fatty acids, succinate, or lactate [6, 7]. Metabolomic profiling thus appears to be highly suitable for studying the effects of CRYO treatment on cardiac metabolism. Specifically, understanding the metabolic traits of CRYO treatment enables inferences to be drawn regarding the metabolic pathways associated with cardiovascular benefits. Although previous metabolomic approaches in small sample studies of left atrial appendage closure in patients with AF have yielded important insights, studies on the metabolic signatures of CRYO have not been evaluated [8, 9]. Accordingly, this study was aimed primarily at using untargeted metabolomics to explore whether CRYO treatment in patients with paroxysmal AF might affect metabolic signatures.

[a]These authors contributed equally to this work
Correspondence: Lilei Yu, MD, PhD, FACC, FESC and Hong Jiang, MD, PhD, FACC, Department of Cardiology, Renmin Hospital of Wuhan University, No. 238 Jiefang Road, Wuhan City, Hubei Province 430060, P.R. China, Tel: +86-27-88041911; Fax: +86-27-88040334, E-mail: lileiyu@whu.edu.cn; hong-jiang@whu.edu.cn

Methods

Study Population

An investigator-initiated, observational clinical trial was conducted at Wuhan University's Renmin Hospital. Patients with documented symptomatic paroxysmal AF were enrolled from October 2021 to January 2022. The patients underwent a first catheter ablation procedure with CRYO. Before enrollment in the trial, patients with paroxysmal AF were required to have had at least one episode of AF documented by an electrocardiogram during the previous year. Before the procedure, each patient underwent medical history taking, physical examination, assessment of arrhythmia symptoms, medication review, 12-lead ECG, transthoracic echocardiography, and transesophageal echocardiography. The two main requirements for study inclusion were a left ventricular ejection fraction $\geq 50\%$ and an anteroposterior left atrium diameter < 5.0 cm.

Detailed Inclusion and Exclusion Criteria

The exclusion criteria included persistent AF, secondary AF, cardiac procedures or implants, heart failure, coronary heart disease, structural heart disease, stroke or transient ischemic attack within 6 months, pericarditis or pericardial effusion, and malignant tumors. Patients provided signed informed consent forms before the procedure. The Renmin Hospital's Ethics Committee at Wuhan University approved this study (approval No. WDRY2021-K147).

Cryoballoon Ablation Procedure

Subclavian vein and right femoral artery punctures, and the coronary sinus and ventricular electrodes were placed. After atrial septal puncture, a 28-mm cryoballoon catheter (Arctic Front Advance,

Medtronic, Minneapolis, USA) was advanced through the left atrium with a 15-Fr deflectable catheter over the wire. A spiral mapping catheter was placed in the targeted pulmonary vein, and the cryoballoon was placed at the pulmonary vein ostium. Under fluoroscopic guidance, the balloon was inflated, and venography was performed to confirm pulmonary vein occlusion, which was identified as the endpoint of ablation (Figure 1). Each pulmonary vein was administered two freezing procedures with targeted ablation times of 180 s. The superior vena cava underwent phrenic nerve pacing to ensure nerve integrity.

Blood Sample Preparation

All participants were required to fast for at least 8 h before sampling in both blood draws. Venous blood was collected from patients with AF before CRYO and 24 hours after CRYO for further analysis. Venous blood samples were collected into tubes. Within 30 min, blood samples were inverted five to eight times and centrifuged (3000 rpm, 15 min at 4 °C), and the serum was isolated and stored at −80 °C until analysis.

Serum Nerve Injury Marker Detection

Serum neurofilament light (NFL), glial fibrillary acidic protein (GFAP), S-100 protein beta chain (S100B), and brain fatty acid-binding protein (B-FABP) were measured with commercial ELISA kits (CUSABIO BIOTECH CO., Ltd., Wuhan, China) according to the manufacturer's instructions.

Untargeted Metabolomic Profiling

After serum samples for metabolomic analysis were collected, 100 µL of blood was quenched in 300 µL of precooled methanol and acetonitrile (2:1, v/v). Each sample had internal standards added as a quality control measure. Samples were subjected to vacuum freeze-drying after 1 minute of vortex mixing. They were then resuspended in 150 µL 50% methanol and centrifuged for 30 min at 4000 rpm to separate the supernatants, which were then injected into a liquid chromatography-mass spectrometry (LC-MS) system. To evaluate the reproducibility of the entire LC-MS analysis, we prepared a quality control (QC) sample by pooling the same volume of each sample.

The metabolites were separated and detected with a Waters 2D UPLC system (Waters, USA) coupled

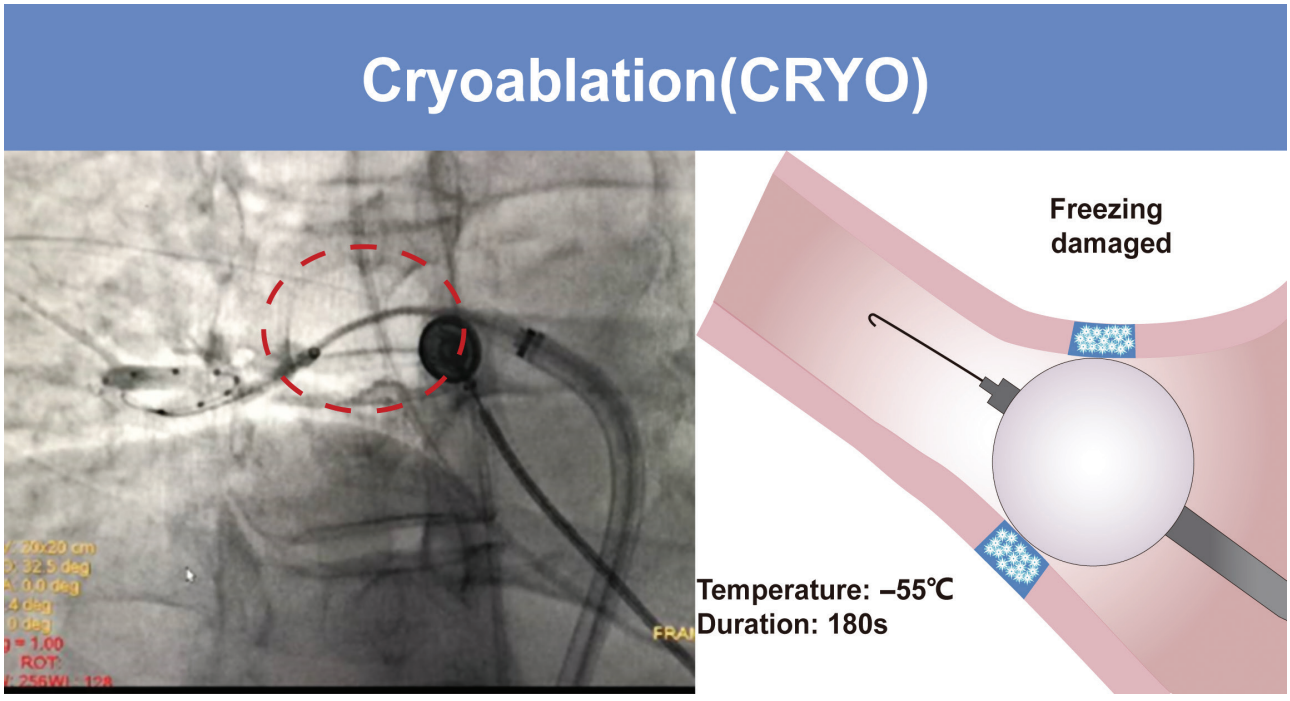

Figure 1 Catheter Ablation Technologies.
(A) Fluoroscopic image depicting the cryoballoon catheter positioned at the pulmonary vein ostium. (B) Illustration depicting the principal design of the cryoballoon.

to a Q Exactive high-resolution mass spectrometer (Thermo Fisher Scientific, USA). LC separation was performed on a Waters ACQUITY UPLC BEH C18 column (1.7 µm, 2.1 mm × 100 mm, Waters, USA). The binary gradient model of the high-performance liquid chromatography system was used to maintain the column temperature at 45 °C. For sample analysis, positive and negative ion modes were used with spray voltages of 3.8 kV and 3.2 kV, respectively. The mass scanning range was 70–1050 m/z, with a resolution of 70,000, and the automatic gain control target for MS acquisitions was set to 3e6 with a maximum ion injection time of 100 ms. The nitrogen sheath gas and nitrogen auxiliary gas flow rates were set to 40 L/min and 10 L/min, respectively. The pooled QC sample was initially injected five times to ensure system equilibrium. For further monitoring of the system's stability, QC samples were interspersed every ten samples.

LC-MS Data Processing

Compound Discoverer 3.0 software (Thermo Fisher Scientific, USA) was used to measure the peak characteristics of relevant metabolites. Peak extraction, peak grouping, retention time correction, peak alignment, and metabolite identification were performed in the data processing and analysis workflow. For data quality assurance, QC sample analysis included investigation of the overlap in base peak chromatograms (BPCs), principal component analysis (PCA), peak lift quantity, and peak response intensity. Through comparison of the exact molecular mass data (m/z) of the samples with those from the database, we identified the metabolites with the online mzCloud and HMDB databases. To understand the functional properties of various metabolites, and identify the primary biochemical metabolic pathways and signal transduction pathways in which the metabolites were involved, we performed metabolic pathway enrichment analysis of differential metabolites between groups with the Kyoto Encyclopedia of Genes and Genomics (KEGG) database.

Statistical Analysis

Categorical variables are presented as numbers and percentages, whereas continuous variables are presented as mean ± standard deviation (SD). Shapiro–Wilk test was used for small samples to assess normality. Depending on the data normality, independent continuous variables were compared with either independent-sample parametric tests (paired Student's t-test) or non-parametric tests (paired Wilcoxon signed-rank test). One-way analysis of variance with Tukey's multiple comparisons test was used to assess the significance of differences among multiple time points. To search for differential metabolites between groups, a combination of multivariate statistical analysis (PCA and partial least squares-discriminant analysis (PLS-DA)), univariate analysis (fold change [FC] and paired Wilcoxon signed-rank test) was used. Significant differential metabolites were identified on the basis of $P < 0.05$, $FC < 0.83$ or > 1.2, and $VIP > 1$. After $\log_2$-log conversion and Pareto scaling with seven-fold cross-validation, the PLS-DA model was created. Heat maps were constructed to show the standardized abundance data for each metabolite, and phenotype analysis was used to group significantly distributed metabolites. Pearson correlation analysis was performed between significant differential serum metabolites and clinical indicators. GraphPad Prism 9 (GraphPad Software, San Diego, CA, USA) or R (http://www.R-project.org, 4.2.2.) was used for statistical analyses. $P < 0.05$ was considered statistically significant.

Results

Baseline Patient Characteristics and Procedural Data

Baseline patient characteristics were shown in Table S1. The mean age was 60.0 ± 12.3 years, and 60% of patients were men. The mean left ventricular ejection fraction was 59.4 ± 1.8%, and the mean left atrial diameter was 3.9 ± 0.5 cm. Table S2 provides an overview of the procedures' characteristics. Of the ten patients, 100% (40 of 40 PVs) met the primary feasibility endpoint of complete acute PVI, and no adverse events were attributed to CRYO. The mean total procedure time was 68.0 ± 14.0 min, and the mean fluoroscopy time was 18.5 ± 5.6 min.

Changes in Metabolites Associated with CRYO in Patients with AF

After screening compounds with a relative peak area CV of 30% more in QC samples, we identified 3755 and 1744 features in positive and negative modes, respectively, in the non-targeted metabolomic profiling (Figure S1A). The PCA of the pooled QC samples clustered together, and the BPC of all QC samples showed substantial overlap (Figure S1B), thus demonstrating the reliability and stability of the LC-MS findings. Figure 2A, B illustrates how PLS-DA distinguished the pre- and post-CRYO groups in both positive and negative modes. Serum levels of metabolites (Figure 2C) distinguished post-CRYO from pre-CRYO patients, on the basis of statistical analysis. A total of 79 metabolites were identified with the KEGG and HMDB databases (Table S3). The heat map and hierarchical clustering analysis illustrated the distribution patterns of differential metabolites between groups (Figure 2D). With an FC of 41.0491, tyramine was among the most significant differential metabolites. Furthermore, we conducted correlation analysis with the *corrplot package* to reveal the potential interactions among the identified compounds, wherein metabolites tended to cluster together in the correlation matrix (Figure S2).

Differential Metabolite Identification and Pathway Analysis

To explore the identities and functional enrichment of differential features, we entered the above differential metabolites as input data to perform the class identification and pathway enrichment analysis by using the HMDB and KEGG databases. As shown in Figure 3A, B, the differential features were significantly associated with lipid

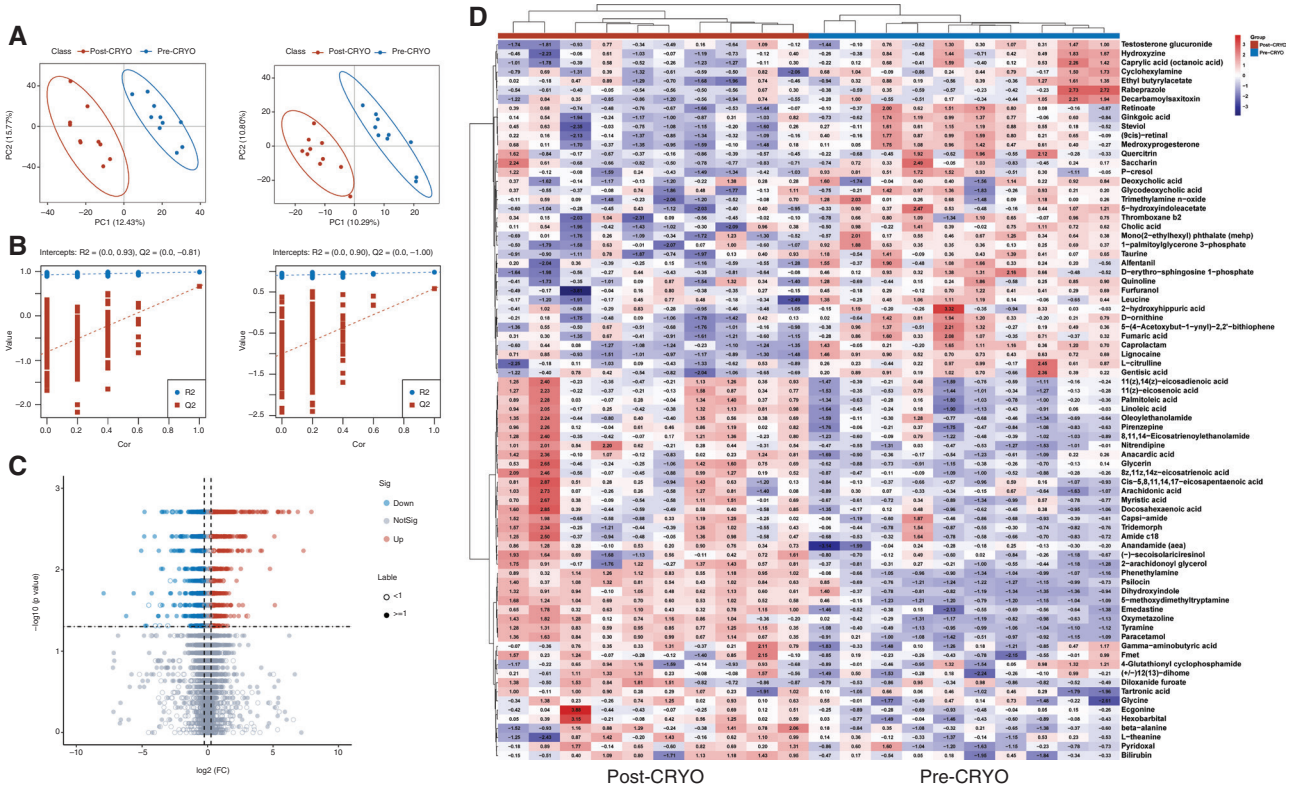

Figure 2 Non-Targeted Metabolomic Profiling Analysis of Human Serum.
(A, B) PLS-DA score plots pre- and post-CRYO in patients with AF. Validation plots of 200 permutation tests in positive mode (left) and negative mode (right) are shown. (C) Volcano plot of differential metabolites. Red, blue, and gray indicate increased, decreased, and non-significant differential metabolites, respectively. VIP > 1, FC < 0.83 or > 1.2, and P < 0.05 were considered to indicate significant differences. (D) Hierarchical clustering heat map of the identified metabolites. Rows indicate metabolites, and columns indicate sample group.

metabolism; amino acid metabolism; and signaling molecules and interactions. The relevant molecules were primarily fatty acyls, alpha-amino acids, peptides, and benzene and substituted derivatives. Pathway analysis was then performed to reveal detailed functional annotation through the *clusterProfiler package*, which indicated that the differential metabolites after CRYO were enriched in pathways including biosynthesis of unsaturated fatty acids, retrograde endocannabinoid (eCB) signaling, neuroactive ligand-receptor interaction, thermogenesis, and linoleic acid metabolism (Figure 3C). To visualize the changes in the levels of metabolites involved in these differential pathways, we constructed a functional annotation heat map (Figure 3D). All differential metabolites (arachidonic acid (AA), 8z, 11z, 14z-eicosatrienoic acid [dihomo-gamma-linolenic acid DGLA], 11(z), 14(z)-eicosadienoic acid, 11(z)-eicosenoic acid, cis-5, 8, 11, 14, 17-eicosapentaenoic acid (EPA), docosahexaenoic acid (DHA), and linoleic acid) involved in unsaturated fatty acid biosynthesis pathways were consistently increased. AA, DGLA, linoleic acid, and (±)12(13)-dihome (Figure S3) participated in linoleic acid metabolism. Furthermore, eight differential metabolites were involved in the neuroactive ligand-receptor interaction pathway, among which tyramine notably increased after CRYO. Interestingly, gamma-aminobutyric acid (GABA), 2-arachidonoyl glycerol (2-AG), and anandamide (AEA) were also associated with retrograde eCB signaling, and, together with glycerin, significantly increased after CRYO.

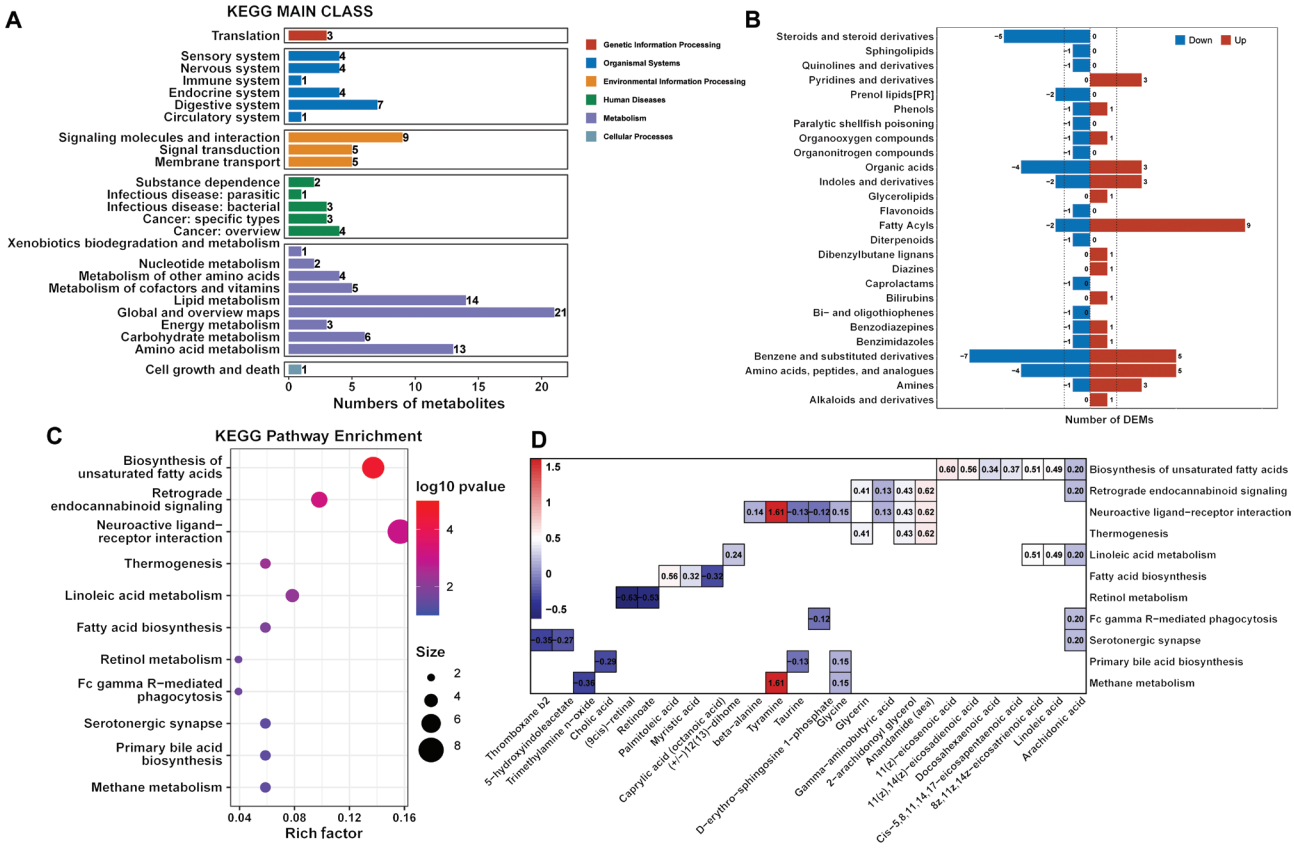

Figure 3 Differential Metabolite Identification and Pathway Analysis.
(A, B) Differential metabolomic profiling annotation with KEGG and HMDB database searching and metabolic network analysis. (C) KEGG pathway enrichment analysis showing altered metabolic pathways of differential metabolites. Each circle represents a pathway, and the size and color of each circle indicate the enriched counts and significance of the pathway, with red indicating the most significant changes after ablation. (D) Functional annotation heat map of the metabolites in altered pathways. Rows indicate pathways, and columns indicate metabolites. The color coding indicates the FC in the differentially present compound. Black indicates the FC of metabolites after $\log_{10}$-log conversion.

Relative Changes in Individual Metabolites After CRYO

To focus on the main disrupted pathways, we further investigated the abundance of metabolites involved in these pathways. We observed significantly elevated unsaturated fatty acids after CRYO treatment. Specifically, the related detected metabolites were polyunsaturated fatty acids (PUFAs) belonging to the omega-6 and omega-3 series (Figure 4). Retrograde signaling is the principal mode through which eCBs mediate short- and long-term plasticity at both excitatory and inhibitory synapses (Figure 5A). After CRYO, levels of the inhibitory neurotransmitter GABA increased. In addition, AA and AEA, the most relevant and prevalent regulators of synaptic function, increased after CRYO. These two CBs were further degraded into AA and GC, both of which were consistently elevated in the post-CRYO group (Figure 5C–G). Furthermore, a series of differential neuroactive ligands were involved in the neuroactive ligand-receptor interaction pathway (Figure 5B), including decreased D-erythro-sphingosine1-phosphate (D-erythro-S1P), and taurine, as well as increased GABA, 2-AG, tyramine, AEA, glycine, and β-alanine (Figure 5E–L). Among these

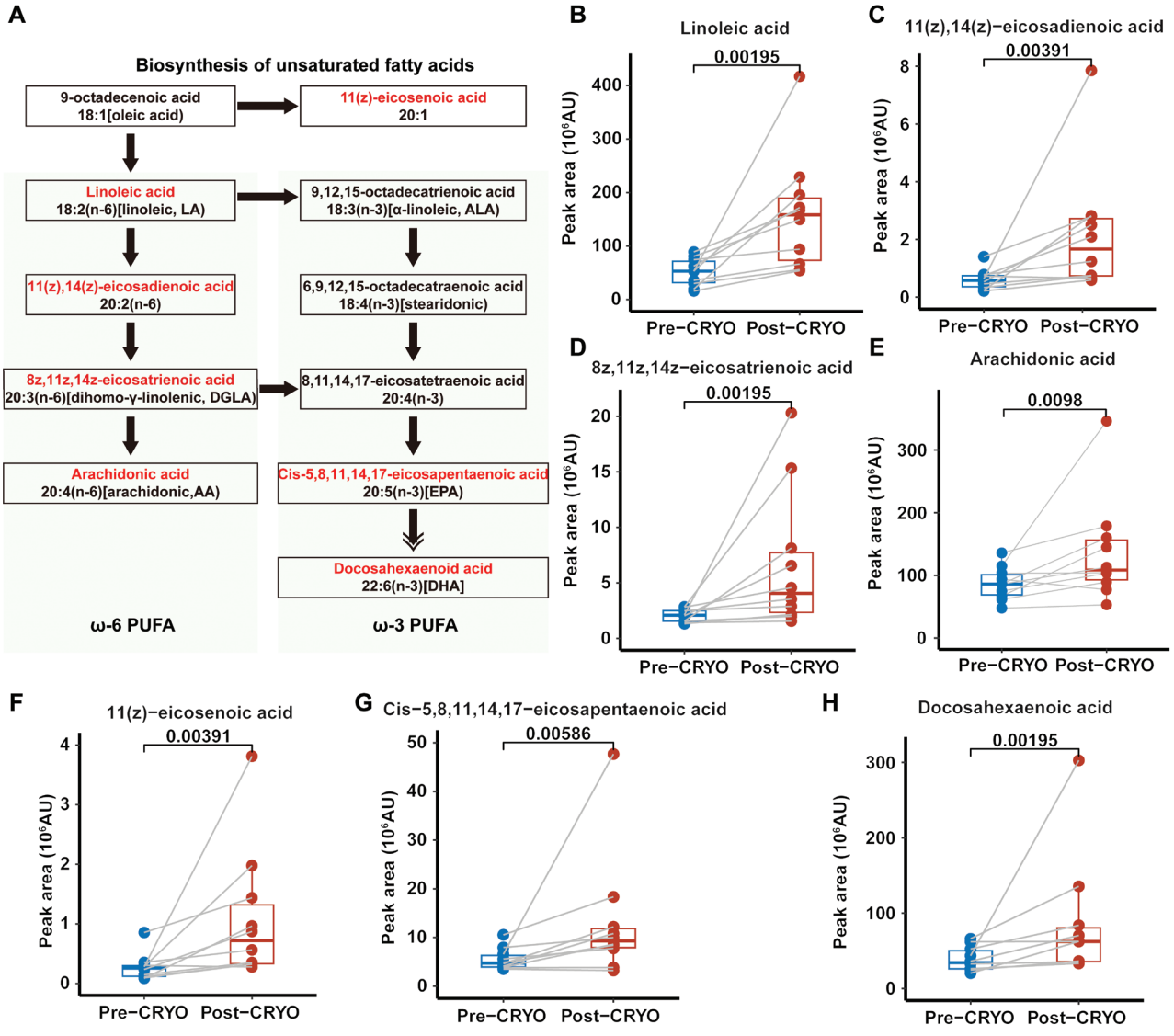

Figure 4 Differential Metabolites Involved in Unsaturated Fatty Acid Biosynthesis.
(A) Schematic representations of biosynthesis of unsaturated fatty acids; significant differential metabolites are shown in red. (B–H) Box and dot plot profiles of the differential PUFAs. PUFA, polyunsaturated fatty acids.

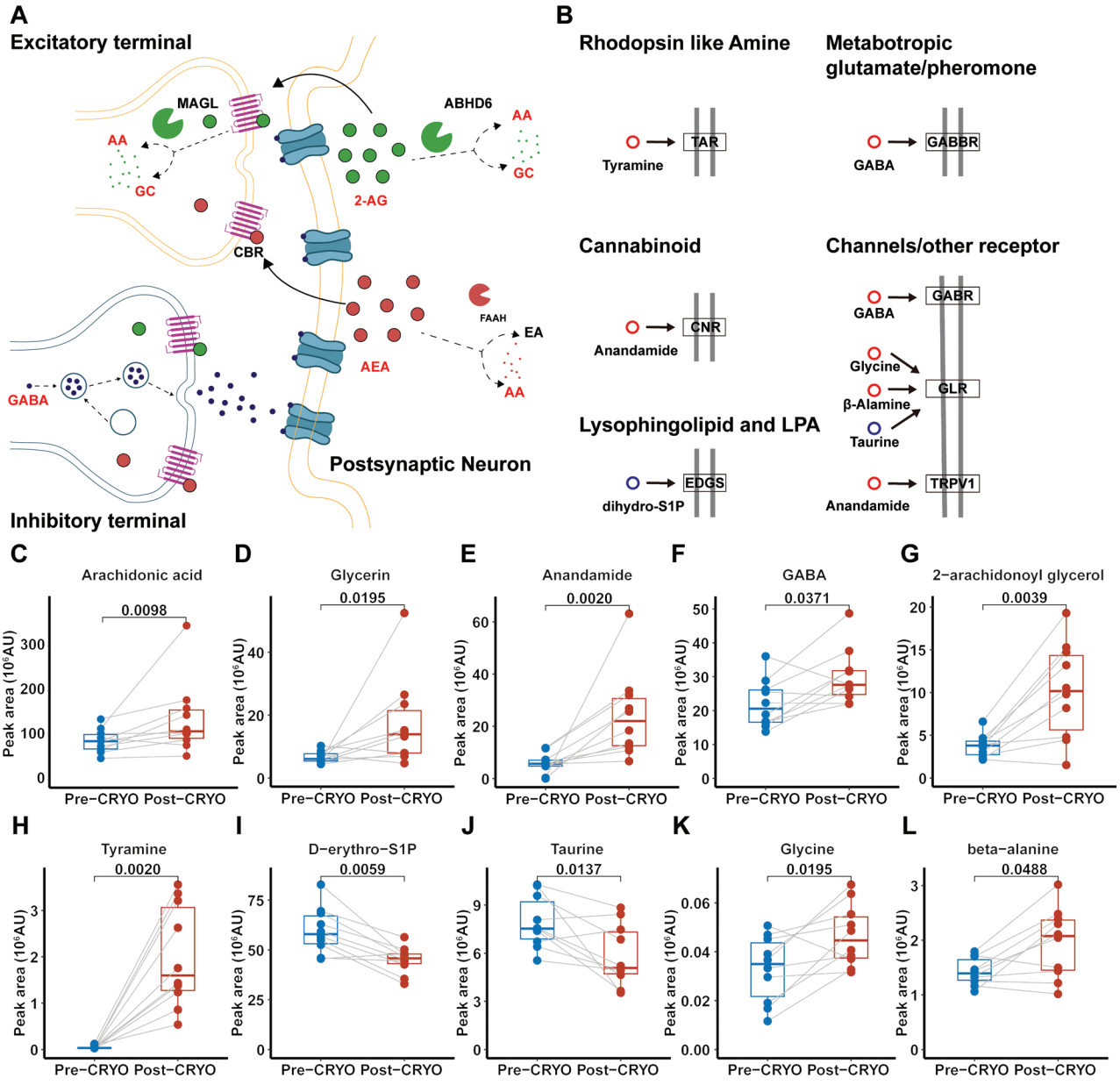

Figure 5 Differential Metabolites Involved in Neuroactive Ligand-Receptor Interaction and Retrograde Endocannabinoid Signaling.

(A) Illustration of the neuroactive ligand–receptor interaction pathway. Red and blue circles represent increasing and decreasing features, respectively. (B) Pattern of retrograde endocannabinoid signaling and metabolism. In brief, postsynaptic activity leads to the production of eCBs, such as 2-AG and AEA, which move backward across the synapse, bind presynaptic CBRs, and suppress neurotransmitter release. These molecules are further degraded into AA and GC. GABA, gamma-aminobutyric acid; 2-AG, 2-aeachidonoyl glycerol; AEA, anadamide; AA, arachidonic acid; GC, glycerin; eCBs: endocannabinoids; CBRs: cannabinoid receptors. (C–L) Box and dot plots of abundance of metabolites involved in neuroactive ligand-receptor interaction and retrograde endocannabinoid signaling.

metabolites, tyramine showed the most significant change. We hypothesized that CRYO therefore might affect neural function. We tested this hypothesis by analyzing neural injury biomarkers across samples from patients with AF pre- and post-CRYO. As expected, the levels of serum neurofilament light (NFL), GFAP, S100B, and B-FABP significantly increased both immediately and 24 h after CRYO (Figure S4). To gain insight into the involvement of these metabolites in all differential pathways, we confirmed correlations among differential metabolites, neural injury biomarkers, and clinical indicators with Pearson's correlation coefficient (r) (Figure 6). In the subgroup analysis,

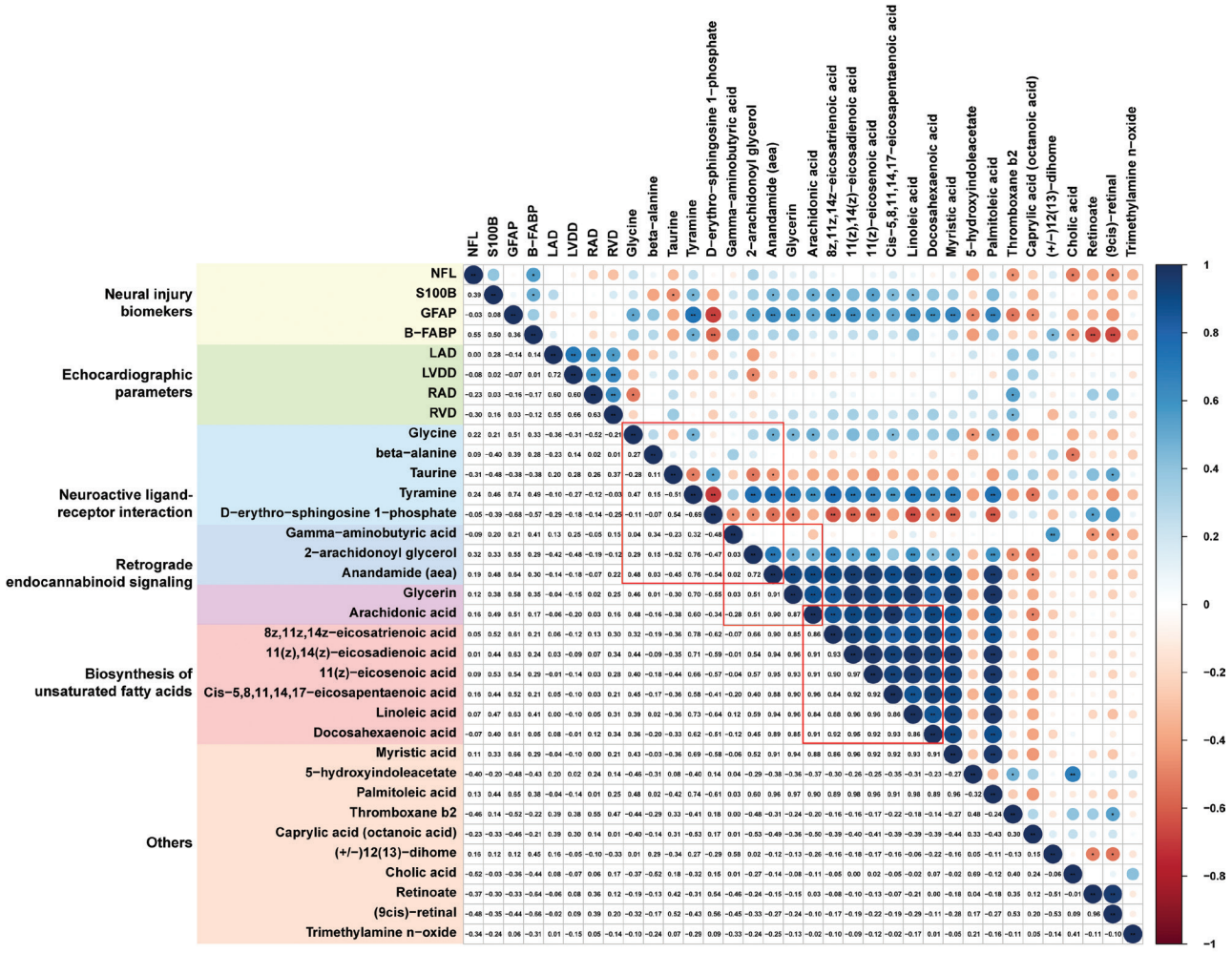

Figure 6 Correlation Analysis among Differential Metabolites in Pathways and Clinical Indicators.
Correlation analysis among differential metabolites, classical neural injury biomarkers and echocardiography parameters. Pearson correlation coefficients between pairs of compounds are shown in the lower left corners of the panels. Six subgroups are shown with frames in different colors. In the upper right corners, the degree of correlation and P values are shown for each pair. Red and blue indicate negative and positive correlations, respectively. $^{*}P < 0.05$; $^{**}P < 0.01$.

seven differential PUFAs showed strong associations ($0.971 > r > 0.838$ and $P < 0.001$). Metabolites associated with retrograde eCB signaling (except GABA) showed highly positive correlations ($0.911 > r > 0.51$ and $P < 0.05$). In addition, five metabolites associated with neuroactive ligand-receptor interaction, such as taurine, tyramine, D-erythro-S1P, and 2-arachidonoyl glycerol, clustered and showed high correlations ($0.898 > r > 0.715$ or $-0.692 < r < -0.509$, and $P < 0.05$). Interestingly, the above metabolites strongly correlated with the seven PUFAs. D-erythro-sphingosine 1-phosphate was negatively correlated with FUFAs ($-0.645 < r < -0.41$), whereas tyramine ($0.779 > r > 0.576$), 2-AG ($0.661 > r > 0.395$), AEA ($0.949 > r > 0.885$), glycerin ($0.958 > r > 0.849$), and AA ($0.964 > r > 0.84$) were positively correlated with FUFAs. Moreover, neural injury biomarkers, particularly GFAP and S100B, were significantly positively correlated with tyramine and PUFAs, whereas GFAP and B-FABP were negatively associated with D-erythro-S1P. Among the echocardiographic parameters, only glycine, 2-AG, and thromboxane b2 showed slight correlations. In addition, the level of 2-AG after CRYO ($r = -0.679$, $P = 0.031$, Figure S5) and its relative change ($r = -0.670$, $P = 0.034$, Figure S6) were negatively associated with recurrent AF. These results indicated that the increase in 2-arachidonoyl glycerol after CRYO might have beneficial effects on AF outcomes.

Discussion

In this study, we showed that the CRYO procedure is a cold-stress stimulus that induces systemic changes in the serum metabolome in patients with paroxysmal AF, thus reflecting the whole-body acute response to cryo-balloon ablation in these patients and potentially providing metabolic benefits. The results indicated significant alterations in pathways associated with the biosynthesis of unsaturated fatty acids, retrograde eCB signaling, neuroactive ligand-receptor interaction, thermogenesis, and linoleic acid metabolism after CRYO – findings that may indirectly reflect the effects of successful CRYO. These metabolic changes may be unique to cryoablation, which was not available in previous studies of radiofrequency and other catheter ablation [10, 11]. The identified differential metabolites may be worthy of investigation as candidate biomarkers for monitoring CRYO efficacy in future studies.

Among the known risk factors for AF, obesity and visceral fat accumulation play important roles in stimulating arrhythmogenic substrates and thus predisposing people to AF. Numerous studies have shown that the amount of epicardial adipose tissue and peri-atrial adipose tissue is closely associated with AF development [12, 13]. Epicardial adipose tissue comprises predominantly white adipose tissue, and cold stimulus induces the browning of white adipose tissue and changes white adipose tissue gene expression and lipid metabolism, thereby promoting adaptive thermogenesis [14]. Cold stimulus promotes the secretion of the lipid mediator 12,13-dihome in BAT and consequently stimulates the thermogenic activity of BAT, regulation of lipid metabolism, and amelioration of cardiac function [15, 16]. In this study, we demonstrated that CRYO, a cold stimulus, significantly increased 12,13-dihome levels after ablation, thereby activating BAT thermogenic lipokines, and providing a potential metabolic benefit from CRYO treatment.

The compound 12,13-dihome is an oxylipin. Oxylipins are bioactive lipids derived from the metabolism of PUFAs (omega-6 and omega-3) after the action of mono- or dioxygenases [17, 18]. Omega-6 is a precursor of 12,13-dihome biosynthesis. Linoleic acid, an omega-6 PUFA, is converted to linoleic epoxide through CYP450-dependent metabolism and is finally metabolized to 12,13-dihome by soluble epoxide hydrolase [19]. CRYO significantly alters the metabolism of PUFAs, including increases in AA, DGLA, 11(z), 14(z)-eicosadienoic acid, 11(z)-eicosenoic acid, EPA, DHA, and linoleic acid levels. Therefore, CRYO is likely to stimulate 12,13-dihome synthesis and thus enhance fatty acid uptake by BAT, and stimulate the browning process in white adipose tissue.

PUFAs prevent cardiovascular diseases by regulating serum triglyceride levels, lipoprotein size, inflammation, plaque stability, and arrhythmia risk [20]. A Cochrane review has revealed the effects of the increased omega-6 PUFAs on cardiovascular disease, thereby supporting the benefits in people at high risk of myocardial infarction [21]. In 11 prospective cohort studies of omega-6 (mostly linoleic acid), higher linoleic acid concentrations have been associated with lower risk of all cardiovascular disease outcomes, including cardiovascular disease mortality [22, 23]. In addition, decreased levels of DGLA, an omega-6 PUFA derived from linoleic acid, strongly correlate with poor prognosis of cardiovascular disease [24]. In particular, recent studies have associated higher circulating concentration and dietary intake of omega-6 fats with lower risk of AF among middle-aged or older patients in multi-ethnic populations [25, 26]. In agreement with these findings, our metabolomic profiles showed significant increases in linoleic acid, DGLA, and 11(z),14(z)-eicosadienoic acid in omega-6 PUFAs after CRYO treatment, thus potentially contributing to cardioprotective effects. Notably, the consumption of high proportions of dietary omega-6 versus omega-3 can have deleterious effects, particularly on inflammatory states, yet this concern is not generally supported by research evidence [20].

We also found that CRYO treatment markedly increased omega-3 PUFAs, particularly EPA and DHA. Omega-3 PUFAs are a component of the cardiomyocyte membrane, where they exert not only stabilizing effects but also direct electrophysiological effects [27]. Previous metabolomic analyses have demonstrated significantly diminished EPA in patients with AF [10]. Supplementation with omega-3 PUFAs has been reported to decrease the incidence of AF in various conditions, such as post-cardiac surgery or cardioversion of AF [28, 29].

Omega-3 PUFA decreases both the inducibility of AF and the duration of pacing-induced AF episodes by inhibiting two major mechanisms responsible for maintaining AF: reentry and rapid focal ectopic firing [30]. Moreover, inflammation and the associated immune response contribute to AF onset and maintenance, as well as electrical and structural atrial remodeling in AF [31]. Omega-3 PUFAs are precursors to resolvins, protective proteins, and other inflammation-resolving mediators. New research suggests that these mediators may have strong anti-inflammatory qualities and contribute to decreasing inflammation [32].

In addition, aging increases the risk of AF, particularly associated atrial electrical and structural remodeling [33]. The activity of PUFAs such as linoleic acid, DGLA, EPA, and DHA decreases with age [34]. PUFA levels have been inversely associated with incident AF among older people in a population with the highest risk of AF [35]. Therefore, CRYO may effectively correct disorders of bioactive fatty acids (linoleic acid, DGLA, EPA, and DHA), and consequently prevent AF and metabolic abnormalities associated with aging. Our findings suggested that CRYO-induced changes in the biosynthesis of unsaturated fatty acids might ameliorate the negative effects of AF ablation. Sustained homeostasis of PUFAs may improve AF treatment and long-term prognosis. However, this hypothesis must be verified through additional cohort studies with longer follow-up periods.

Recent studies have suggested that the immunemodulatory lipid-signaling molecules eCBs may provide a missing link between the beneficial effects of PUFAs and the management of cardiometabolic diseases [36]. The eCBs mediate the beneficial effects of omega-3 fatty acids on cardiometabolic disorders, and increased levels of 2-AG and oxylipin enhance the anti-inflammatory effects of omega-3 fatty acids. Activation of the cannabinoid receptor has been shown to stimulate an anti-inflammatory state by increasing anti-inflammatory cytokines and decreasing levels of pro-inflammatory cytokines [37]. In addition, the ability of cannabinoid receptors to fine-tune and regulate GABAergic synaptic transmission through retrograde signaling has been found to inhibit neuronal activity, and neuronal activation plays an important role in the development of AF [37]. Interestingly, our results indicated that the eCB-mediated retrograde signaling pathway was also altered after CRYO, with 2-AG and AEA significantly elevated after ablation, thus potentially decreasing inflammation, and enhancing synaptic function and neurocognitive function.

Prior studies have shown that activation of the cardiac autonomic nervous system is often required for AF triggering and possibly maintenance [38]. Moreover, a recent study has indicated that extensive autonomic denervation alone without PVI is as successful as PVI at maintaining sinus rhythm 1 year postablation [39]. In the present study, we found elevated serum nerve injury markers after CRYO treatment, thus suggesting that freezing may damage the ganglion plexus in the fat pad around the pulmonary vein. KEGG analysis further revealed significant alterations in neuroactive ligand-receptor interaction pathways after CRYO treatment. Neuroactive ligands affect neuronal function by binding intracellular receptors, which in turn bind transcription factors and regulate gene expression [40]. Among them, tyramine, which is associated with tyrosine metabolism, was among the most significant differential metabolites, thus further indicating that CRYO results in neuron injury and affects cardiac sympathetic activity [41]. The cardioprotective effects of neuroactive steroid have been associated with neuroactive ligand-receptor interaction in patients treated with coronary artery bypass graft surgery [42]. In addition, another study has found that neuroactive ligand-receptor interaction is closely associated with arrhythmogenic right ventricular cardiomyopathy [43]. On the basis of these findings, we infer that CRYO might play a crucial role in cardioprotection by affecting the neuroactive ligand-receptor interaction pathway.

This study has several limitations that should be noted. First, this study was cross-sectional, had a small sample size, and lacked a control group without CRYO, thus potentially hindering strong conclusions from being drawn. Therefore, randomized controlled trial studies with larger sample sizes and deeper exploration of relevant mechanisms are required. Second, although untargeted platforms reveal many serum metabolites, the interpretability and quantification of findings are limited. Finally, this study performed the first exploration of the influence of successful CRYO on metabolic profiling and is therefore descriptive and hypothesis-generating.

Ethics Statement

The study adhered to the tenets of the Declaration of Helsinki and was conducted in accordance with the regulations of the Renmin Hospital's Ethics Committee at Wuhan University. The Renmin Hospital's Ethics Committee at Wuhan University approved this study (Approval No. WDRY2021-K147).

Data Availability Statement

The datasets generated and/or analyzed during the current study are not publicly available but are available from the corresponding author upon reasonable request.

Author Contributions

MJX, FDG, and JW: substantial contributions to data acquisition, or data analysis and writing; YJW, ZHL, JX, ZW, and SYW: data collection and revision; LPZ and YYW: drafting the article or critically revising it for important intellectual content. LLY and HJ: conception, design, and supervision. All authors contributed to the article and approved the submitted version.

Acknowledgments

This work was supported by grants from National Natural Science Foundation of China (82241057, 82270532, 81970287, 82100530, and 82200556), and the Foundation for Innovative Research Groups of Natural Science Foundation of Hubei Province, China (2021CFA010).

Conflicts of Interest

Lilei Yu is the Deputy Editor-in-Chief of CVIA. Lilei Yu is not involved in the peer review or decision-making process of the manuscript. The other authors have no competing interests to disclose.

Supplementary Material

Supplementary Materials for this paper can be found at the following link https://cvia-journal.org/wp-content/uploads/2023/11/Revised_supplementary_materials.pdf.

REFERENCES

1. Benjamin EJ, Muntner P, Alonso A, Bittencourt MS, Callaway CW, Carson AP, et al. Heart disease and stroke statistics-2019 update: a report from the American Heart Association. Circulation 2019;139:e56–528.
2. Andrade JG, Wells GA, Deyell MW, Bennett M, Essebag V, Champagne J, et al. Cryoablation or drug therapy for initial treatment of atrial fibrillation. N Engl J Med 2021;384:305–15.
3. Vandenberk B, Lauwers L, Robyns T, Garweg C, Willems R, Ector J, et al. Quality of life outcomes in cryoablation of atrial fibrillation-a literature review. Pacing Clin Electrophysiol 2021;44:1756–68.
4. Andrade JG, Deyell MW, Macle L, Wells GA, Bennett M, Essebag V, et al. Progression of atrial fibrillation after cryoablation or drug therapy. N Engl J Med 2023;388:105–16.
5. Avitall B, Kalinski A. Cryotherapy of cardiac arrhythmia: from basic science to the bedside. Heart Rhythm 2015;12:2195–203.
6. Sugimoto S, Mena HA, Sansbury BE, Kobayashi S, Tsuji T, Wang CH, et al. Brown adipose tissue-derived MaR2 contributes to cold-induced resolution of inflammation. Nat Metab 2022;4:775–90.
7. van Marken Lichtenbelt WD, Vanhommerig JW, Smulders NM, Drossaerts JM, Kemerink GJ, Bouvy ND, et al. Cold-activated brown adipose tissue in healthy men. N Engl J Med 2009;360:1500–8.
8. Fastner C, Behnes M, Sartorius B, Wenke A, Lang S, Yucel G, et al. Interventional left atrial appendage closure affects the metabolism of acylcarnitines. Int J Mol Sci 2018;19:500.
9. Rusnak J, Behnes M, Saleh A, Fastner C, Sattler K, Barth C, et al. Interventional left atrial appendage closure may affect metabolism of essential amino acids and bioenergetic efficacy. Int J Cardiol 2018;268:125–31.
10. Huang K, Wang Y, Bai Y, Luo Q, Lin X, Yang Q, et al. Gut microbiota and metabolites in atrial fibrillation patients and their changes after catheter ablation. Microbiol Spectr 2022;10:e0107721.
11. Li J, Zuo K, Zhang J, Hu C, Wang P, Jiao J, et al. Shifts in gut microbiome and metabolome are associated with risk of recurrent atrial fibrillation. J Cell Mol Med 2020;24:13356–69.

12. Ernault AC, Meijborg VMF, Coronel R. Modulation of cardiac arrhythmogenesis by epicardial adipose tissue: JACC state-of-the-art review. J Am Coll Cardiol 2021;78:1730–45.
13. Wang W, Tian Y, Wang W, Yin H, Yin D, Tian Y. Role of epicardial adipose tissue in triggering and maintaining atrial fibrillation. Cardiovasc Innov Appl 2022;7. doi: 10.15212/cvia.2022.0012.
14. Bartelt A, Bruns OT, Reimer R, Hohenberg H, Ittrich H, Peldschus K, et al. Brown adipose tissue activity controls triglyceride clearance. Nat Med 2011;17:200–5.
15. Lynes MD, Leiria LO, Lundh M, Bartelt A, Shamsi F, Huang TL, et al. The cold-induced lipokine 12,13-diHOME promotes fatty acid transport into brown adipose tissue. Nat Med 2017;23:631–7.
16. Pinckard KM, Shettigar VK, Wright KR, Abay E, Baer LA, Vidal P, et al. A novel endocrine role for the BAT-released lipokine 12,13-diHOME to mediate cardiac function. Circulation 2021;143:145–59.
17. Macedo APA, Munoz VR, Cintra DE, Pauli JR. 12,13-diHOME as a new therapeutic target for metabolic diseases. Life Sci 2022;290: 120229.
18. Leiria LO, Tseng YH. Lipidomics of brown and white adipose tissue: implications for energy metabolism. Biochim Biophys Acta Mol Cell Biol Lipids 2020;1865:158788.
19. Hildreth K, Kodani SD, Hammock BD, Zhao L. Cytochrome P450-derived linoleic acid metabolites EpOMEs and DiHOMEs: a review of recent studies. J Nutr Biochem 2020;86:108484.
20. Schulze MB, Minihane AM, Saleh RNM, Riserus U. Intake and metabolism of omega-3 and omega-6 polyunsaturated fatty acids: nutritional implications for cardiometabolic diseases. Lancet Diabetes Endocrinol 2020;8:915–30.
21. Hooper L, Al-Khudairy L, Abdelhamid AS, Rees K, Brainard JS, Brown TJ, et al. Omega-6 fats for the primary and secondary prevention of cardiovascular disease. Cochrane Database Syst Rev 2018;11:CD011094.
22. Jakobsen MU, O'Reilly EJ, Heitmann BL, Pereira MA, Balter K, Fraser GE, et al. Major types of dietary fat and risk of coronary heart disease: a pooled analysis of 11 cohort studies. Am J Clin Nutr 2009;89:1425–32.
23. Farvid MS, Ding M, Pan A, Sun Q, Chiuve SE, Steffen LM, et al. Dietary linoleic acid and risk of coronary heart disease: a systematic review and meta-analysis of prospective cohort studies. Circulation 2014;130:1568–78.
24. Nilsen DWT, Myhre PL, Kalstad A, Schmidt EB, Arnesen H, Seljeflot I. Serum levels of dihomo-gamma (γ)-linolenic acid (DGLA) are inversely associated with linoleic acid and total death in elderly patients with a recent myocardial infarction. Nutrients 2021;13:3475.
25. Garg PK, Guan W, Nomura S, Weir N, Karger AB, Duprez D, et al. Plasma omega-3 and omega-6 PUFA concentrations and risk of atrial fibrillation: the multi-ethnic study of atherosclerosis. J Nutr 2021;151:1479–86.
26. Tajik B, Tuomainen TP, Isanejad M, Salonen JT, Virtanen JK. Serum n-6 polyunsaturated fatty acids and risk of atrial fibrillation: the Kuopio Ischaemic Heart Disease Risk Factor Study. Eur J Nutr 2022;61: 1981–9.
27. Christou GA, Christou KA, Korantzopoulos P, Rizos EC, Nikas DN, Goudevenos JA. The current role of omega-3 fatty acids in the management of atrial fibrillation. Int J Mol Sci 2015;16:22870–87.
28. Calo L, Bianconi L, Colivicchi F, Lamberti F, Loricchio ML, de Ruvo E, et al. N-3 fatty acids for the prevention of atrial fibrillation after coronary artery bypass surgery: a randomized, controlled trial. J Am Coll Cardiol 2005;45:1723–8.
29. Kumar S, Sutherland F, Morton JB, Lee G, Morgan J, Wong J, et al. Long-term omega-3 polyunsaturated fatty acid supplementation reduces the recurrence of persistent atrial fibrillation after electrical cardioversion. Heart Rhythm 2012;9: 483–91.
30. Laurent G, Moe G, Hu X, Holub B, Leong-Poi H, Trogadis J, et al. Long chain n-3 polyunsaturated fatty acids reduce atrial vulnerability in a novel canine pacing model. Cardiovasc Res 2008;77:89–97.
31. Hu YF, Chen YJ, Lin YJ, Chen SA. Inflammation and the pathogenesis of atrial fibrillation. Nat Rev Cardiol 2015;12:230–43.
32. Mozaffarian D, Wu JH. Omega-3 fatty acids and cardiovascular disease: effects on risk factors, molecular pathways, and clinical events. J Am Coll Cardiol 2011;58:2047–67.
33. Lin YK, Chen YA, Lee TI, Chen YC, Chen SA, Chen YJ. Aging modulates the substrate and triggers remodeling in atrial fibrillation. Circ J 2018;82:1237–44.
34. Das UN. "Cell Membrane Theory of Senescence" and the role of bioactive lipids in aging, and aging associated diseases and their therapeutic implications. Biomolecules 2021;11:241.
35. Wu JH, Lemaitre RN, King IB, Song X, Sacks FM, Rimm EB, et al. Association of plasma phospholipid long-chain omega-3 fatty acids with incident atrial fibrillation in older adults: the cardiovascular health study. Circulation 2012;125:1084–93.
36. Saleh-Ghadimi S, Kheirouri S, Maleki V, Jafari-Vayghan H, Alizadeh M. Endocannabinoid system and cardiometabolic risk factors: a comprehensive systematic review insight into the mechanistic effects of omega-3 fatty acids. Life Sci 2020;250:117556.
37. Haspula D, Clark MA. Cannabinoid receptors: an update on cell signaling, pathophysiological roles and therapeutic opportunities in neurological, cardiovascular, and inflammatory diseases. Int J Mol Sci 2020;21:7693.
38. Chakraborty P, Po SS. The role of autonomic denervation in the success of atrial fibrillation ablation: can pulsed-field ablation

provide the answer? Heart Rhythm 2023;20:341–2.
39. Kim MY, Coyle C, Tomlinson DR, Sikkel MB, Sohaib A, Luther V, et al. Ectopy-triggering ganglionated plexuses ablation to prevent atrial fibrillation: GANGLIA-AF study. Heart Rhythm 2022;19:516–24.
40. Wei J, Liu J, Liang S, Sun M, Duan J. Low-dose exposure of silica nanoparticles induces neurotoxicity via neuroactive ligand-receptor interaction signaling pathway in zebrafish embryos. Int J Nanomedicine 2020; 15:4407–15.
41. Yu Z, Wang L, Wu S, Zhao W. Dissecting the potential mechanism of antihypertensive effects of RVPSL on spontaneously hypertensive rats via widely targeted kidney metabolomics. J Sci Food Agric 2023;103:428–36.
42. Wang J, Cheng J, Zhang C, Li X. Cardioprotection effects of sevoflurane by regulating the pathway of neuroactive ligand-receptor interaction in patients undergoing coronary artery bypass graft surgery. Comput Math Methods Med 2017;2017:3618213.
43. Chen P, Long B, Xu Y, Wu W, Zhang S. Identification of crucial genes and pathways in human arrhythmogenic right ventricular cardiomyopathy by coexpression analysis. Front Physiol 2018;9:1778.